

## Sr–Nd isotopic compositions of Paleoproterozoic metavolcanic rocks from the southern Ashanti volcanic belt, Ghana

Samuel DAMPARE\*<sup>\*\*\*</sup>, Tsugio SHIBATA\*, Daniel ASIEDU<sup>\*\*\*</sup>, Osamu OKANO\*, Johnson MANU<sup>\*\*\*</sup> and Patrick SAKYI<sup>\*\*\*</sup>

*\*Department of Earth Sciences, Okayama University, 1-1, Tsushima-Naka 3-Chome, Okayama 700-8530, Japan*

*\*\*National Nuclear Research Institute, Ghana Atomic Energy Commission, P.O. Box LG 80, Legon-Accra, Ghana*

*\*\*\*Department of Earth Science, University of Ghana, P.O. Box LG 58, Legon-Accra, Ghana*

Neodymium (Nd) and strontium (Sr) isotopic data are presented for Paleoproterozoic metavolcanic rocks in the southern part of the Ashanti volcanic belt of Ghana. The metavolcanic rocks are predominantly basalts/basaltic andesites and andesites with minor dacites. Two types of basalts/basaltic andesites (B/A), Type I and Type II, have been identified. The Type I B/A are stratigraphically overlain by the Type II B/A, followed by the andesites and the dacites. The analyzed volcanic rocks commonly have low initial  $^{87}\text{Sr}/^{86}\text{Sr}$  ratios consistent with previous studies on Paleoproterozoic rocks from the West African craton. The LREE-depleted, tholeiitic Type I B/A exhibit back-arc basin geochemical signatures and show high positive epsilon Nd (i.e.,  $\epsilon_{\text{Nd}}(2.1\text{ Ga}) = +3.89$  to  $+7.21$ ), which suggest a long term depleted source and also indicate that they were produced in an entirely oceanic environment devoid of influence of continental crust. The isotope signatures are thus consistent with the previously published trace element data of the Type I basalts/basaltic andesites in suggesting that their parent magma was generated from a depleted mantle. The Type I B/A have Nd model ages ( $T_{\text{DM2}}$ ) of 1.83–2.09 Ga similar to their formation ages, suggesting that they were juvenile at their time of formation. The andesites and the Type II B/A andesites show LREE-enriched patterns and exhibit characteristics of subduction zone-related magmas, and show initial  $\epsilon_{\text{Nd}}(2.1\text{ Ga})$  values of  $-1.15$  to  $+1.35$  and Nd model ages ( $T_{\text{DM2}}$ ) of 2.32–2.58 Ga. The LREE-enriched dacitic porphyry also exhibits characteristics of subduction zone-related magmas, and have initial  $\epsilon_{\text{Nd}}(2.1\text{ Ga})$  value of  $-2.24$  and Nd model ages ( $T_{\text{DM2}}$ ) of 2.64 Ga. The Nd isotopic data confirms the juvenile character of the Birimian crust, but also suggests some contributions of a pre-Birimian crustal material (or Archean?) in the genesis of some of the metavolcanic rocks. Our isotopic result is consistent with the island arc complex model which views Paleoproterozoic terranes of West Africa in the context of subduction–accretion processes.

**Keywords:** Sr–Nd isotopes, petrogenesis, tectonic setting, Birimian metavolcanics, Ashanti volcanic belt

### I. Introduction

The processes involved in crustal evolution/growth of continents over geologic time and the nature of the material extracted from the mantle to produce the protocrust, especially during the Archean and Proterozoic, have been surrounded with controversies. While some believe that continental crust grows through time by accretion of island arcs, others are of the view that crustal growth may have resulted from remelting of sinking mafic bodies in a geodynamic context devoid of plate tectonics, underplating of rift/ocean island magmas or eruptions of continental flood basalts (references in Abouchami et al., 1990). The

Archean–Proterozoic boundary (which is arbitrarily put at 2.5 Ga) is considered as a major marker in the changes of the style of crustal evolution in the earth's history. Researches carried out in the greenstone belts of Precambrian shields of Canada, the southwestern United States, western Australia, Greenland, Scandinavia, southern Africa and southern India tend to agree with this major change (cf. Sylvester and Attoh, 1992), thereby supporting the assertion of a worldwide, fundamental change in crust-mantle evolution at the Archean–Proterozoic boundary.

Studies of the Paleoproterozoic 'Birimian' rocks of the Leo-Man shield of the West African Craton (WAC;

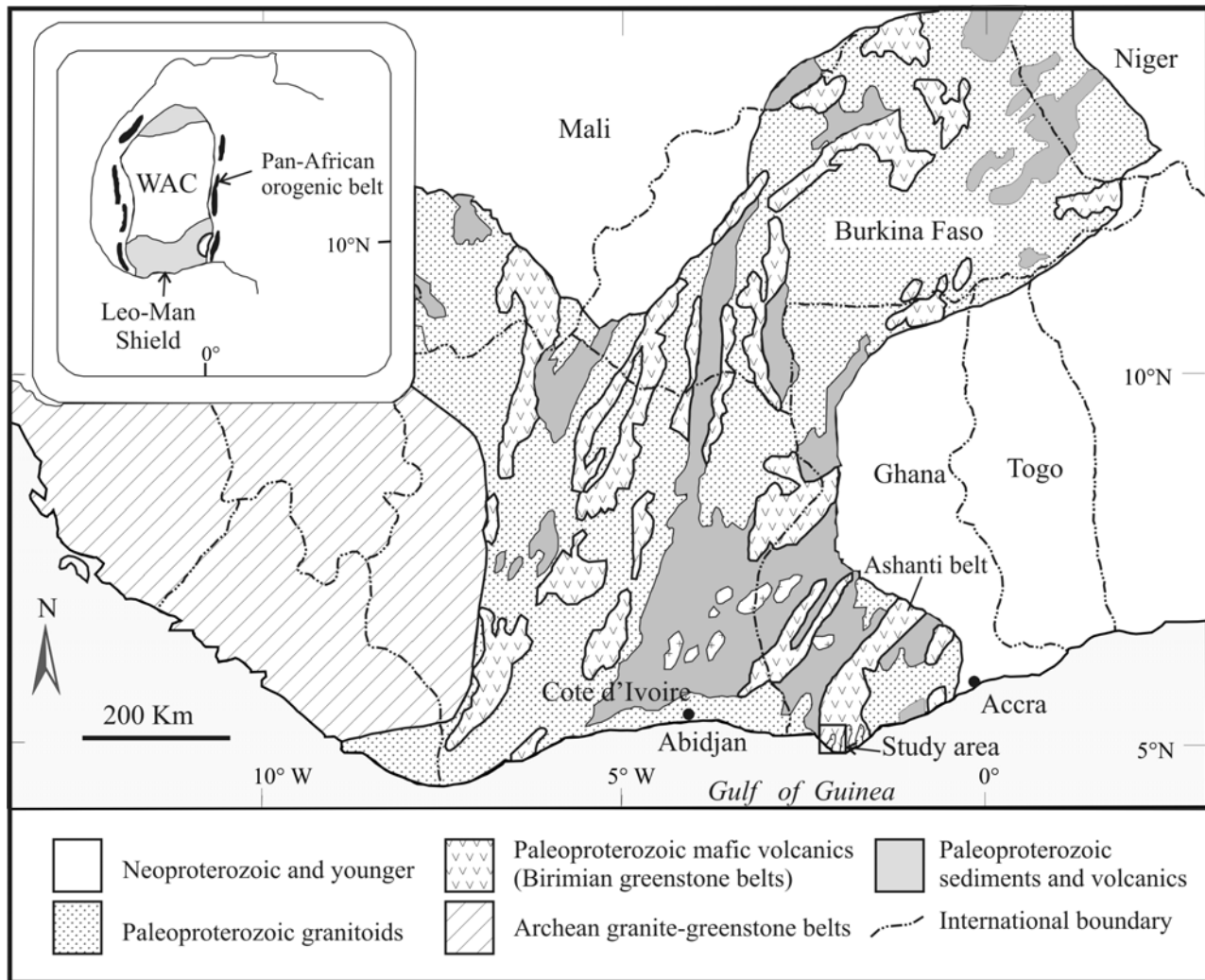


Fig. 1. Geologic sketch of the Leo-Man shield of the West Africa craton (WAC; inset) showing the Paleoproterozoic (Birimian) greenstone belts and the location of the study area (adopted after Attoh et al., 2006).

Fig. 1) have, however, yielded interesting and provocative findings for reconsideration of models regarding the geodynamic evolution of greenstone belts of Precambrian shields. For instance, the ~2.1 Ga Birimian magmatism in the West Africa craton took place between 2.4 and 1.9 Ga, thus bridging a major gap in mantle activity and crustal evolution for a period thought to be quiescent in the North America–Europe regions (Nelson and DePaolo, 1985; Patchett and Arndt, 1986) and Australia (McCulloch, 1987). It has also been suggested from geochemical studies of the Birimian volcanic rocks (Sylvester and Attoh, 1992) and the metasedimentary rocks (Asiedu et al., 2004) from Ghana that the Birimian terrane of Ghana and probably the West African craton may not conform to

the worldwide fundamental change in the crust–mantle evolution at the Archean–Proterozoic boundary. Understanding the Birimian magmatism in the West African craton could unequivocally be useful in the appraisal of the crustal growth of continents in the earth's evolution history.

The main Paleoproterozoic crustal growth event (or Eburnean orogeny) in the WAC represents a major juvenile crust-forming process with involvement of only a negligible Archean crustal components (e.g., Abouchami et al., 1990; Liégeois et al., 1991; Boher et al., 1992; Taylor et al., 1992; Pawlig et al., 2006). However, the context of crustal accretion and tectonic setting as well as the lithostratigraphic feature of the Paleoproterozoic rocks has been a subject of contrasted

## Sr–Nd isotopic compositions of metavolcanic rocks

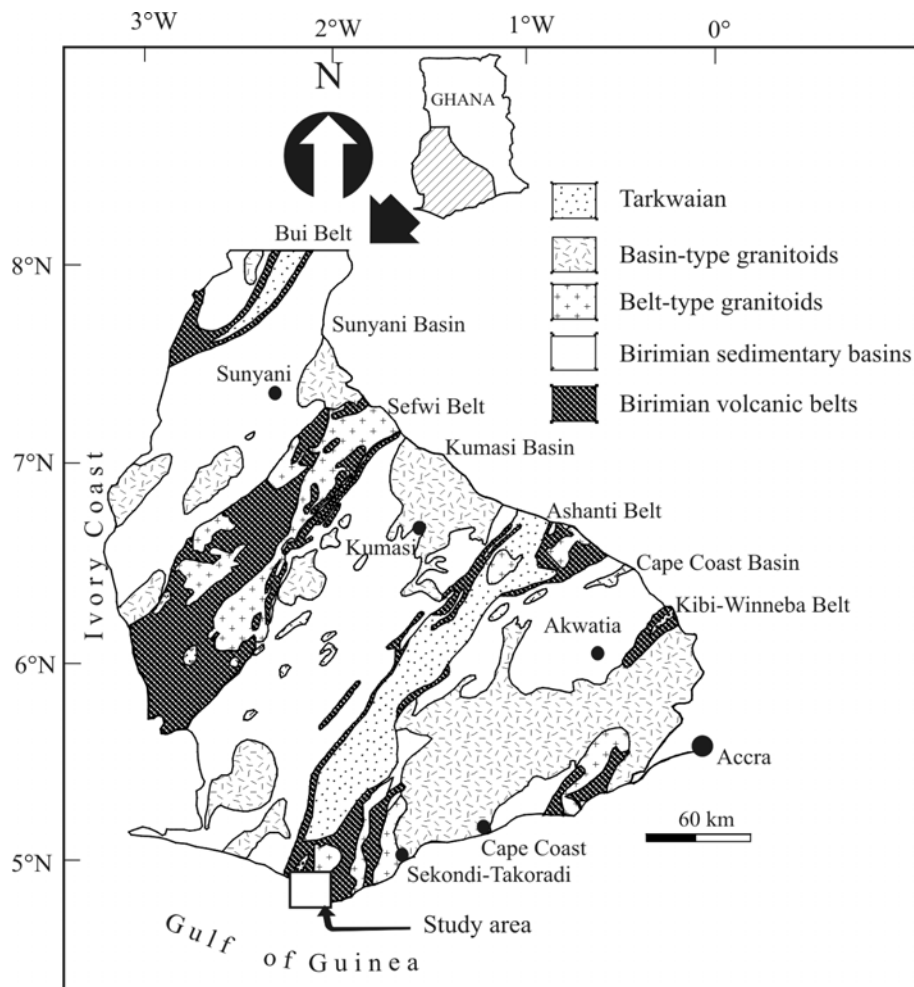


Fig. 2. Simplified geological map of Ghana showing the study area.

interpretations. The lithostratigraphic succession of these rocks (i.e., the volcano-sedimentary and bimodal volcanics) has over the years been contentious with respect to whether the sedimentary unit lies below (e.g., Junner, 1940; Milési et al., 1992; Feybesse and Milési, 1994), or above (e.g., Tagini, 1971; Hirdes et al., 1996; Asiedu et al., 2004) the volcanic unit. It is now widely accepted that the two units formed quasi-contemporaneously, as lateral facies equivalents (e.g., Leube et al., 1990). In terms of the tectonic setting in which the rocks were formed, interpretations vary between generation of the Birimian juvenile crust in arc environments (e.g., Sylvester and Attoh, 1992; Mortimer, 1992; Pohl and Carlson, 1993; Asiedu et al., 2004; Dampare et al., 2005) and from plume-related magmatism (e.g., Abouchami et al., 1990; Lompo, 2009). Two main models have been proposed to account for the tectonic processes involved in the formation of the rocks: accretionary orogeny (e.g., Abouchami et al., 1990; Boher et al., 1992; Davis et

al., 1994; Feybesse and Milési, 1994; Hirdes et al., 1996; Ledru et al., 1994; Hirdes and Davis, 2002) versus transcurrent tectonics models (e.g., Bassot, 1987; Doumbia et al., 1998; Pouclet et al., 1996).

Available  $^{207}\text{Pb}/^{206}\text{Pb}$  and U–Pb zircon geochronological data on the granitoids intruding the Birimian terrane tend to suggest that Paleoproterozoic crust formation in the West African craton are marked by two successive major episodes of coeval plutonism and volcanism (i.e., Birimian *sensu stricto* followed by Bandamian). A pre-Birimian crustal growth episode has also been suggested by some workers (e.g., Gasquet et al., 2003; Pawlig et al., 2006).

The Paleoproterozoic terrane of Ghana is mainly characterized by northeast–southwest trending volcanic belts with intervening basins, and both the belts and basins are intruded by granitoids of Proterozoic age (Fig. 2). The southern part of the Ashanti greenstone belt, one of the volcanic belts of Ghana, is characterized by three volcanic lobes, made up of basaltic flows,

andesitic lavas, pyroclastic and sedimentary rocks, with granite-diorite plutonic suites occupying intervening positions. Mafic–ultramafic plutonic rocks also occur in this part of the volcanic belt. Some petrographic and geochemical data are available on these rocks (e.g., Sylvester and Attoh (1992; Loh and Hirdes, 1999; Attoh et al., 2006; Dampare et al., 2005; Dampare, 2008; Dampare et al., 2008; Dampare et al., in review). However, isotopic data are for the metavolcanic, granitoids and the mafic–ultramafic rocks. Isotopic studies have mostly been restricted to the granitoids of which U–Pb zircon ages (Taylor et al., 1988, 1992; Hirdes et al., 1992; Opare-Addo, 1993; Loh and Hirdes, 1999; Attoh et al., 2006) and Sr–Nd data (Taylor et al., 1988, 1992) are available. Loh and Hirdes (1999) also determined U–Pb zircon ages of a felsic pyroclastic unit within the volcanic pile.

The objectives of this paper are: (1) to present chemical data of Paleoproterozoic metavolcanic rocks exposed in the southern Ashanti greenstone terrane in southwestern Ghana; and (2) to discuss the petrogenesis and the tectonic setting of the metavolcanic rocks.

## II. Geological setting

Paleoproterozoic rocks, which comprise the bulk of the Birimian terrane of the Leo-Man shield (Fig. 1), form a significant portion of the West African Craton (WAC) to the east and north of the Archean Liberian cratonic nucleus. The Paleoproterozoic terrane is characterized by narrow sedimentary basins and linear, arcuate volcanic belts and intruded by several generations of granitoids (Leube et al., 1990; Hirdes et al., 1996; Doumbia et al., 1998), and corresponds to a period of accretion during the 2.1–2.0 Ga Eburnean orogeny (e.g., Abouchami et al., 1990). The Eburnean tectono-thermal event was accompanied by the deformation and the emplacement of syn- to post-orogenic tonalite–trondhjemite–granodiorite (TTG) and granite plutons along fractures (e.g., Leube et al., 1990; Vidal and Alric, 1994; Feybesse et al., 2006). The event resulted in widespread metamorphism mostly under greenschist-facies conditions (e.g., Oberthür et al., 1998; Béziat et al., 2000). Also, evidence of medium amphibolite-facies metamorphism may be observed in the vicinity of granitoid plutons (e.g., Junner, 1940; Eisenlohr and Hirdes, 1992; Debat et al., 2003).

In Ghana, the Paleoproterozoic supracrustal rocks are subdivided into the Birimian and Tarkwaian. The Birimian rocks comprise a series of subparallel, roughly equal-spaced northeast trending volcanic belts of volcanic rocks separated by an assemblage of sedimentary rocks. The Birimian rocks were

traditionally classified into a two-fold lithostratigraphic and chronological system, consisting of an older metasedimentary sequence (referred to as Lower Birimian) and a younger volcanic sequence of predominantly tholeiitic basalt and pyroclastic rocks (referred to as Upper Birimian) (e.g., Junner, 1940). Leube et al. (1990) have indicated that the volcanic and sedimentary rock sequences formed contemporaneously as lateral facies equivalents. The Birimian rocks are overlain by the detrital Tarkwaian sedimentary rocks in almost all the prominent volcanic belts, and both formations were subjected to similar deformation events, which involved compression along a southeast–northwest trending axis (Eisenlohr and Hirdes, 1992; Blenkinsop et al., 1994). The Tarkwaian rocks are made up of conglomerates, sandstones and subordinate shale, with much of the clastic material in the sediments derived from the adjacent Birimian units (Tunk et al., 2004). Two main suites of granitoids, namely the Dixcove- (or belt-type) and Cape Coast-type (or basin-type) granitoids, intrude the Birimian terrane of Ghana. The metaluminous, relatively Na-rich, Dixcove-type granitoids, which are dominantly hornblende- to biotite-bearing granodiorite to diorite, monzonite and syenite, intrude the Birimian volcanic belts and they may be coeval with the volcanic rocks (Eisenlohr and Hirdes, 1992). The Cape Coast-type granitoids, which are predominantly peraluminous, two-mica granodiorites, with lesser hornblende- and biotite-bearing granodiorites, are emplaced within the Birimian sedimentary basins. The Dixcove granitoids have been dated at  $2172 \pm 1.4$  Ma in the Ashanti Belt (Hirdes et al., 1992) and the Cape Coast type between  $2104 \pm 2$  and  $2123 \pm 3$  Ma in the Kumasi Basin (Oberthür et al., 1998). Other types of granitoids include the localized, biotite and hornblende Winneba granitoids, and the K-rich Bongo granitoids which cut the Tarkwaian rocks in the volcanic belts. The Cape Coast-, Kumasi-, Dixcove- and Bongo-type granitoids have strong mantle affinities whereas the Winneba-type has an Archean sialic precursor (Sm–Nd model age of  $\sim 2.6$  Ga) (Taylor et al., 1992). The Winneba-type granitoids are believed to be the only rock suite in Ghana which show evidence for a significant magmatic contribution from an Archean continental crust in their genesis.

Tectonic evolution models proposed for the Paleoproterozoic rocks of Ghana have commonly considered two deformation events. In the first event, the Birimian rocks were deformed and intruded by granitoid, and was later uplifted and eroded. The erosional products deposited in a series of grabens located within the volcanic belts to form the Tarkwaian. During the second event, which involved renewed folding (cf. Moon and Mason, 1967; Ledru et al., 1988)



## Sr–Nd isotopic compositions of metavolcanic rocks

or gravity tectonic processes (Leube et al., 1990), both the Birimian and Tarkwaian were deformed. Recently, however, it has been suggested that both the Birimian and Tarkwaian were subjected to a single, progressive deformation event, which involved compression along a southeast-northwest trending axis, resulting in folding and thrusting with subsequent flattening and localized oblique-slip shearing (e.g., Eisenlohr, 1992; Eisenlohr and Hirdes, 1992; Blenkinsop et al., 1994; Allibone et al., 2002). Also, the tectonic setting in which the Paleoproterozoic rocks of Ghana formed is contentious, and interpretations of tectonic models for the Birimian terrane of Ghana basically varies between the intracratonic rift setting and island arc complexes. Leube et al. (1990) have proposed an intracontinental rift model for the Paleoproterozoic rocks, whereas arc or subduction related models are preferred by some other workers (Sylvester and Attoh, 1992; Pohl and Carlson, 1993; Loh and Hirdes, 1999; Asiedu et al., 2004; Dampare et al., 2005; Attoh et al., 2006; Dampare et al., 2008). Feybesse et al. (2006) developed a metallogenesis model for the occurrence of gold deposits in Ghana which invoked a combination of continental margin, juvenile magmatism and convergence and collision between an old continent and a juvenile crust for the tectonic environments in which the Birimian greenstone belts were generated. Thus, the Ashanti volcanic belt probably marks the boundary between an Archean continental domain and a Birimian oceanic domain. For Harcouet et al. (2007), the basement in the Ashanti area is likely to be of continental type rather than oceanic, as the results of their numerical modeling using thermal parameters such as thermal conductivity values and heat-production rates are more consistent with the continental basement scenario. In terms of crustal growth event, Taylor et al. (1992) have indicated, from geochronological and isotopic data, that the Birimian of Ghana represents a major early Proterozoic magmatic crust-forming event around 2.3–2.0 Ga by differentiation from a slightly depleted mantle source. Thus, the Birimian of Ghana forms part of the major Proterozoic (Eburnean) episode of juvenile crustal accretion which is recognized in West African Craton and dated at 2.2–2.1 by Abouchami et al. (1990). Davis et al. (1994), also following the accretionary model, have proposed that the Birimian sedimentary basins resulted from accretion of arcs and oceanic plateaus now represented by allochthonous Birimian volcanic belts. Feybesse et al. (2006) have suggested that the evolution of the Paleoproterozoic province of Ghana began around 2.35–2.30 Ga with plutonic activity and the deposition of banded iron formation (BIF)-bearing volcanogenic sediments in basins. According to the authors, the Birimian volcanic belts correspond to a

major period of accretion of juvenile basic volcanic–plutonic rocks to an Archean continental domain around 2.25–2.17 Ga, whereas the Birimian sedimentary activity occurred at 2.15–2.10 Ga.

The southern portion of the Ashanti volcanic belt forms three branches referred to as the Axim branch, Cape Three Points branch and Butre branch, with three plutons (locally termed as Prince's Town, Dixcove and Ketan pluton) occupying positions between these branches (Loh and Hirdes, 1999). The volcanic branches are composed of basaltic and andesitic lavas, and pyroclastic rocks. The bulk of these andesitic rocks occur in the Axim volcanic branch where they probably occupy a stratigraphically upper position in the volcanic sequence of the southern Ashanti belt (Loh and Hirdes, 1999). Several mafic–ultramafic rocks are associated with the volcanic rocks in the southern Ashanti volcanic belt (Fig. 2).

Economically, gold and manganese occur in the southern Ashanti belt. Some of the gold deposits are structurally-controlled and mostly occur in the transition zones between the volcanic belts and the basin sediments (e.g., Kesse, 1985; Leube et al., 1990; Hirdes et al., 1993; Oberthür et al., 1996). The two most important regional structural controls of the gold deposits in the southern Ashanti belt seem to be the Axim high-strain zone along the western flank of the Ashanti belt, and the sheared granitoid/greenstone settings (Loh and Hirdes, 1999). The gold-bearing quartz-pebble conglomerates of the Tarkwaian also contribute to the gold production from the volcanic belt. Studies carried out on gold mineralization in the Ashanti belt have suggested that the gold-bearing fluids are coeval with (peak-greenschist-facies metamorphism (e.g., Mumin and Fleet, 1995; Loh and Hirdes, 1999). It has also been indicated that higher grade mineral assemblages are mostly restricted to the contact aureoles of the belt type granitoids (e.g., Junner, 1935; Leube et al., 1990). Recently, John et al. (1999), on the basis of mineral chemistry, have suggested that the entire Ashanti belt of southeastern Ghana underwent epidote–amphibolite–facies metamorphism ( $T = 500\text{--}650\text{ }^{\circ}\text{C}$  and  $P = 5\text{--}6\text{ kbar}$ ) before experiencing retrograde metamorphism under the greenschist-facies conditions.

### III. Previous geochronology and isotopic studies

Isotopic data on Paleoproterozoic rocks from Ghana are generally scarce and the few available geochronological data from southwestern Ghana have been summarized by Pigios et al. (2003). On the basis of Sm–Nd whole-rock isochron and model ages, Taylor et al. (1992) constrained the age of Birimian supracrustal rocks of western Ghana to  $2166 \pm 66\text{ Ma}$ .

Most radiometric dating on the Birimian of Ghana indicates that volcanic belts were deposited between 2250 and 2186 Ma whereas the sediments were deposited 100–60 Ma later into basins (Leube et al., 1990; Davis et al., 1994; Oberthür et al., 1998; Pigois et al., 2003). Feybesse et al. (2006), however, suggested that the Birimian volcanic belts corresponded to a major period of accretion of juvenile basic volcanic–plutonic rocks to an Archean continental domain around 2.25–2.17 Ga, whereas the Birimian sedimentary activity occurred at 2.15–2.10 Ga. Using SHRIMP II U–Pb analyses of detrital zircons, Pigois et al. (2003) constrained the maximum age of sedimentation of the Tarkwaian, which overlie the Birimian rocks, to  $2133 \pm 4$  Ma. The Birimian and Tarkwaian rocks host the major gold deposits in Ghana, with most of the gold deposits concentrated along the western flank of the Ashanti belt. The major epigenetic lode-gold event occurred late in the Eburnean orogeny, after the peak of metamorphism was reached (Oberthür et al., 1998; John et al., 1999; Yao et al., 2001; Pigois et al., 2003). Using hydrothermal rutile, Oberthür et al. (1998) have obtained the age of hydrothermal alteration to be  $2092 \pm 3$  and  $2086 \pm 4$  Ma. Recently, Pigois et al. (2003) have determined the most robust age of  $2063 \pm 9$  Ma for gold mineralization in Ghana from SHRIMP II U–Pb analyses of hydrothermal xenotime.

Previous isotopic works on rocks from the southern Ashanti volcanic belt include the contributions from Taylor et al. (1988, 1992), Hirdes et al. (1992), Opare-Addo (1993), Loh and Hirdes (1999) and Attah et al. (2006). Most of these studies have been restricted to the granitoids, and the age of the metavolcanic rocks are mainly constrained by the ages of the granitoids. Opare-Addo et al. (1993) reported precise TIMS U–Pb zircon ages of  $2172 \pm 4$  Ma for the migmatites and granitoids from the Ketan pluton, which is located to the eastern margin of the Butre branch. Hirdes et al. (1992) obtained a precise TIMS U–Pb zircon age of  $2174 \pm 2$  Ma for a tonalite from the Dixcove pluton, which outcrops between the Butre and the Cape Three Points volcanic branches. Taylor et al. (1988, 1992) reported initial  $^{87}\text{Sr}/^{86}\text{Sr}$  ratio of  $0.7017 \pm 8$ , source  $^{238}\text{U}/^{204}\text{Pb}$  (model) of 7.84 and Sm–Nd model age ( $T_{\text{DM}}$ ) of 2.20–2.24 Ga for the Dixcove pluton, and concluded that the rocks were largely juvenile in character. Attah et al. (2006) have recently determined TIMS U–Pb zircon ages of  $2159 \pm 4$  Ma for a granodiorite from the Prince's Town pluton, which occupies the intervening position between the Cape Three Points and the Axim branches. The age obtained for the Prince's Town pluton is younger than the ones yielded by the Dixcove and Ketan plutons and consistent with the post-tectonic field relations of the Prince's Town pluton, which typically shows well-preserved, undeformed,

magmatic textures (Attah et al., 2006). The age of the Prince's Town pluton has constrained a minimum age for the Aketakyi ophiolitic complex, as it intrudes the western flank of the complex. Loh and Hirdes (1999) obtained TIMS U–Pb zircon ages of  $2266 \pm 2$  Ma for a felsic pyroclastic unit within the volcanic pile. According to the authors, these high zircon values could probably indicate the presence of early Birimian volcanic activity. Dampare et al. (in review) have recently carried out Sr–Nd isotopic studies of the ultramafic and mafic rocks as well as the Prince's Town pluton, and they have provided Nd isotopic evidence for a possible contamination of the juvenile Birimian crust of the southern Ashanti belt by a significant amount of a pre-Birimian crustal material (or Archean?).

#### IV. Field relations and petrography

A detailed description of the field relations among the various rocks of the southern Ashanti volcanic belt is provided by Loh and Hirdes (1999). The volcanic rocks, mainly composed of basaltic and andesitic lavas, and pyroclastic rocks, form three major NE–SW trending lobes/branches referred to from east to west as the Butre branch, Cape Three Points branch and the Axim branch with three granitoid intrusives (locally called the Prince's Town, Dixcove and Ketan pluton) occurring at intervening positions between them (Fig. 3). The Butre branch consists predominantly of massive, pillow basalt flows; the Cape Three Points branch is characterized by interlayered pyroclastic rocks, basaltic flows and small subvolcanic intrusions, with pyroclastics being more prominent than flows whereas the Axim branch consists of interlayered volcanics and pyroclastic rocks in roughly even proportions, with more than 50% of the volcanics being of andesitic composition (Loh and Hirdes, 1999). The lithostratigraphy of the southern Ashanti volcanic belt is poorly established. According to Loh and Hirdes (1999), the volcanic rocks of the Butre branch form the bottom part of the total volcanic pile, followed by that of the Cape Three Points branch, and the volcanic rocks of the Axim branch occupy the upper stratigraphic position. There is, however, a problem with this stratigraphy, as it cannot explain the overall synclinal structure of the Ashanti volcanic belt (Dampare et al., 2008). For Sylvester and Attah (1992), the volcanic pile of the Dixcove belt (same as the Cape Three Points volcanic branch) consists of 500m of pillow breccias and hyaloclastites at the base, 3000m of pillowed, massive lava flows in the middle, and 1000m of aquagene tuffs interbedded with massive flows at the top, capped by a manganese-oxide and

## Sr–Nd isotopic compositions of metavolcanic rocks

manganese-carbonate deposit, but this has been questioned by Loh and Hirdes (1999).

Ultramafic to mafic complexes as well as isolated mafic bodies are associated with this greenstone–granitoid belt. The ultramafic–mafic rocks occur as two discrete bodies, i.e., Aketakyi ultramafic complex (UMC) and Ahama ultramafic body. The Ahama ultramafic body was first discovered and mapped by Loh and Hirdes (1999). It is located in the area of the headwaters of the Ahama stream in the Axim volcanic branch. The rocks are poorly exposed. The Ahama rocks are predominantly pyroxenites. The Aketakyi UMC, which was previously mapped by Bartholomew (1961) and Loh and Hirdes (1999), has recently been studied by Attoh et al. (2006). The rocks are well exposed on the coast and form a jagged coastline from Aketakyi to Cape Three Points. The western contact of the Aketakyi UMC is marked by a fault and considered to represent the lower section of the complex, where it is made up of ~2.0 km thick zone of coarse-grained peridotites, including harzburgite and

dunite (Attoh et al., 2006). The rocks are variably serpentinized and altered to various degrees. Layering in the ultramafic complex appears to follow the regional northeast strike of the volcanic belt. This layering is more pronounced in the gabbroic rocks, which occur in the eastern contact zone. Rodingite has been identified in the ultramafic rocks. The mafic bodies include the Axim gabbro, Kegyina gabbro and gabbroic rocks from the Aketakyi area. Although the gabbroic rocks have not been dated, they appear to have different origins as well as emplacement records. According to Loh and Hirdes (1999), most of the gabbroic rocks appear to predate the Eburnean tectono-thermal event. The Axim gabbro is associated with argillite and andesitic lavas in the transition zone between the Kumasi basin and the Ashanti belt. The rocks are massive and show various degrees of alteration. The Kegyina gabbro is poorly exposed and deeply weathered. It is located within the Prince's Town pluton toward its margin, and probably represents the mafic boarder of the Prince's Town pluton (Loh and Hirdes,

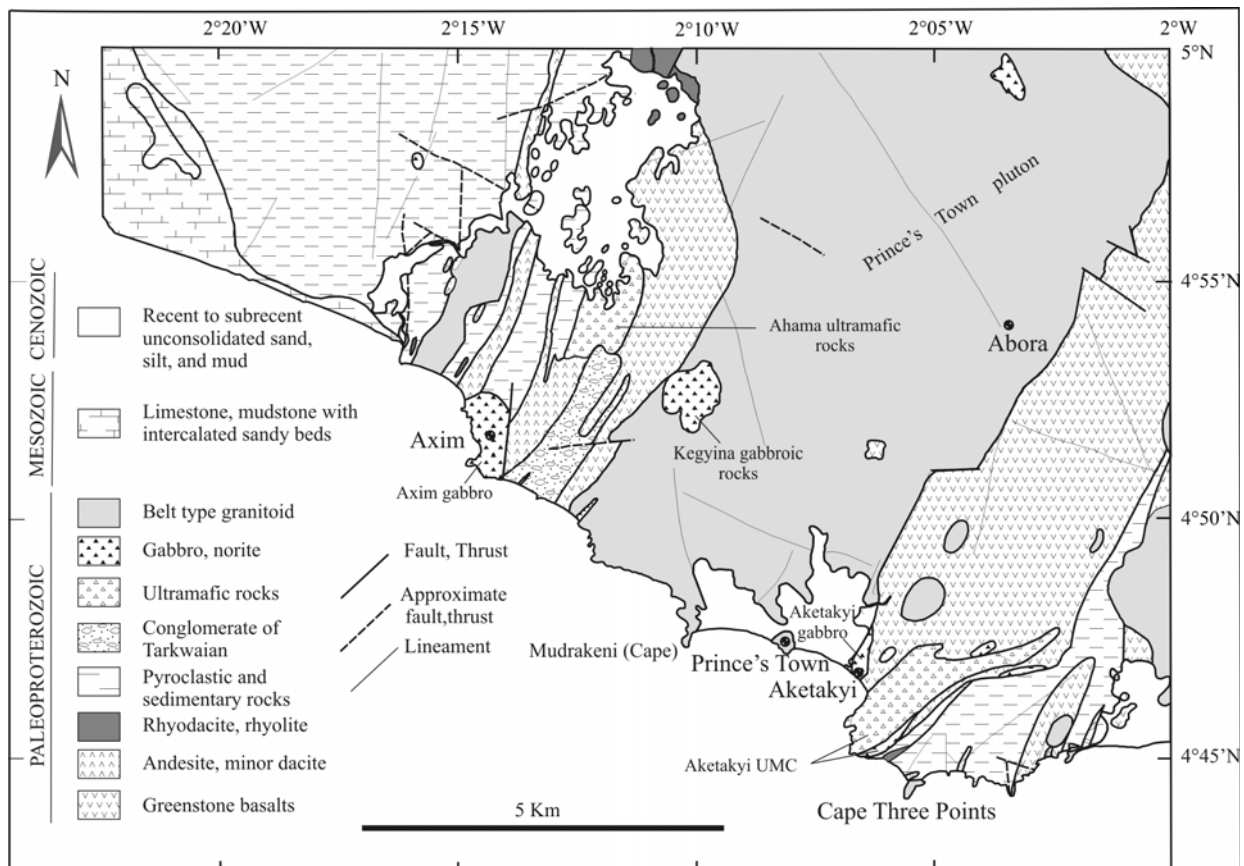


Fig. 3. Geological map of the southern Ashanti volcanic belt of Ghana showing the Axim (left) and Cape Three Points (right) volcanic branches (after Loh and Hirdes, 1999).



1999). The rocks are coarse-grained and massive. The gabbroic body, which intrudes the area north of Aketakyi town, is considered as an equivalent of the Kegyina gabbro. This body is made up of fine- to coarse-grained types. The Aketakyi gabbroic rocks are associated with the Aketakyi ultramafic complex, and they commonly occur as strongly foliated rocks at the outer flanks of the ultramafic complex. The ultrabasic nature of some analyzed gabbroic rocks led Loh and Hirdes (1999) to suggest that the gabbroic rocks could be part of the main Aketakyi ultramafic complex, and Attoh et al. (2006) have also indicated that these rocks represent the upper section of the ultramafic complex. The gabbroic zone of the Aketakyi ultramafic complex is stratigraphically overlain by a sheeted-dyke complex, which consists of basaltic hyaloclastites intercalated with fine-grained sediments including chert and disrupted basaltic-andesitic sills. The ultramafic complex with the overlying sheeted-dyke complex and associated volcanics has been suggested to represent a cross-section of a Paleoproterozoic oceanic crust (Attoh et al. 2006).

Metavolcanic rocks, mainly andesitic and basaltic lavas flows, were collected from the Axim and the Cape Three Points volcanic branches of the southern Ashanti greenstone belt for this study (Fig. 3). The analyzed basalts/basaltic andesites are dark green to dark grey, fine-grained and massive. They are mostly aphyric and sparsely porphyritic, with less than 10% phenocrysts set in a microcrystalline groundmass. The primary minerals of the basalts/basaltic andesites comprise mainly plagioclase and pyroxene which are either partially or completely replaced by actinolite and epidote. Plagioclase which occurs as euhedral to subhedral phenocrysts is usually replaced by epidote and sericite, and in some cases by albite and calcite. Relict pyroxene is observed in some of the specimens. The groundmass consists of lath-like and microlite plagioclase, and secondary quartz, carbonate, chlorite and sericite. Apatite, magnetite and ilmenite occur as the main accessory minerals. Leucoxene may occur as an alteration product of ilmenite. In the foliated types, some whitish bands made up of mainly quartz, calcite and albite alternate with dark greenish bands consisting of chlorite, epidote and actinolite.

The andesites and some dacites were collected from the Axim branch. They are greenish to dark grey, fine- to medium-grained and massive. The andesites are mostly microporphyritic. Plagioclase constitutes the main phenocryst phase in the rocks. Some of the phenocrysts might be originally a mafic mineral which is now replaced by actinolite, chlorite, epidote and sometimes carbonate. Euhedral to subhedral plagioclase crystals are commonly replaced by epidote. The fine-grained groundmass consists mainly of

plagioclase, and secondary actinolite, epidote and quartz. Accessory minerals include opaques and apatite, with the opaques sometimes altering to leucoxene. The dacites show a porphyritic texture with few phenocrysts of plagioclase and quartz set in a fine-grained cryptocrystalline matrix, which consists of secondary sericite, epidote, chlorite, as well as accessory pyrite, ilmenite and apatite.

## V. Analytical methods

Analysis of major elements of the metavolcanic rocks was carried out on fused discs by the automated X-ray fluorescence spectrometer, Philips model PW 1480, at the Department of Earth Sciences, Okayama University. The trace elements analyses of selected samples were performed at the Activation Laboratories Ltd. (Actlabs), Ontario, Canada, using fusion inductively coupled plasma and inductively coupled plasma-mass spectrometry (ICP-MS). Details of the analytical procedures (i.e., accuracy, precision and standards) were presented by Dampare et al. (2008).

Sr–Nd isotope analyses were conducted at the Center of Instrumental Analysis, Okayama University, Japan. Approximately 70 mg of whole-rock powdered samples were dissolved in a mixture of purified  $\text{HNO}_3$ – $\text{HF}$ – $\text{HClO}_4$  in Teflon vials on a hot plate (100–140 °C). Separation of Sr and Nd was carried out using a standard two-column ion-exchange technique, described in detail by Dampare (2008). Isotopic analyses were carried out using a five-collector Finnigan MAT-262 mass spectrometer. Sr and Nd were loaded in 2%  $\text{H}_3\text{PO}_4$  (repeatedly purified using a cation exchange column) on double Ta-Re filaments and analyzed in the static mode. In order to correct for mass fractionation, the  $^{87}\text{Sr}/^{86}\text{Sr}$  and  $^{143}\text{Nd}/^{144}\text{Nd}$  isotopic data were normalized against the values of  $^{86}\text{Sr}/^{88}\text{Sr} = 0.1194$  and  $^{146}\text{Nd}/^{144}\text{Nd} = 0.7219$ , respectively. The mean value of the measured  $^{87}\text{Sr}/^{86}\text{Sr}$  ratios of NBS 987 standard was  $0.710295 \pm 11$  ( $2\sigma$ ;  $n=13$  analyses). The mean of the measured  $^{143}\text{Nd}/^{144}\text{Nd}$  ratios of JNdi-1 standard gave  $0.5121428 \pm 9$  ( $2\sigma$ ;  $n=5$  analyses), which corresponds to a La Jolla Nd standard value of 0.511885.

## VI. Geochemistry

Detailed chemical compositions of the southern Ashanti belt metavolcanic rocks have been discussed elsewhere (Dampare et al., 2008), and a summary of these compositions is provided in Table 1. Two types of basalts/basaltic andesites (B/A), Type I and Type II, have been identified with respect to their geochemical features. The Type I B/A, obtained from the Cape Three Points greenstone branch, are characterized by  $\text{SiO}_2$



## Sr–Nd isotopic compositions of metavolcanic rocks

Table 1

Summary of whole-rock major and trace element compositions of metavolcanic rocks from the southern Ashanti volcanic belt

| Locality                       | Cape Three Points Volcanic Branch                  |                                  | Axim Volcanic Branch                                |                                       |
|--------------------------------|--|----------------------------------|---|---------------------------------------|
|                                | Type I Basalts/<br>Basaltic andesites <sup>a</sup> | Dacitic<br>porphyry <sup>b</sup> | Type II Basalts/<br>Basaltic andesites <sup>a</sup> | Andesites and<br>Dacites <sup>a</sup> |
| (wt.%)                         |  |                                  |   |                                       |
| SiO <sub>2</sub>               | 47.56?51.76  | 62.71                            | 48.48–52.87   | 54.16–68.13                           |
| TiO <sub>2</sub>               | 0.62?0.82  | 0.37                             | 0.54–0.86   | 0.35–0.77                             |
| Al <sub>2</sub> O <sub>3</sub> | 12.57?14.53  | 14.86                            | 10.41–16.17   | 13.47–16.14                           |
| Fe <sub>2</sub> O <sub>3</sub> | 10.35?12.03  | 5.61                             | 8.59–9.93   | 4.32–9.36                             |
| MnO                            | 0.17?0.19  | 0.08                             | 0.13–0.15   | 0.07–0.18                             |
| MgO                            | 6.85?8.16  | 3.39                             | 3.99–12.67  | 0.99–5.05                             |
| CaO                            | 6.08?10.76   | 4.91                             | 6.94–9.00   | 2.95–7.60                             |
| Na <sub>2</sub> O              | 0.90?3.19  | 4.86                             | 2.26–4.51   | 2.35–5.10                             |
| K <sub>2</sub> O               | 0.02?0.31  | 0.32                             | 0.98–1.22   | 0.34–2.49                             |
| P <sub>2</sub> O <sub>5</sub>  | 0.06?0.11  | 0.09                             | 0.17–0.30   | 0.09–0.28                             |
| Mg#                            | 54.1?60.0  | 54.5                             | 47.9–71.6   | 31.1–53.5                             |
| (ppm)                          |  |                                  |   |                                       |
| V                              | 224?277  | 104                              | 168–275   | 105–202                               |
| Cr                             | 670?750  | 290                              | 250–1060  | 160–270                               |
| Co                             | 31?70  | 20                               | 35–42   | 30–48                                 |
| Ni                             | 220?330  | 130                              | 100–260   | 40–120                                |
| Cu                             | 40?130   | 70                               | 30–180  | 30–70                                 |
| Zn                             | 70?100   | < 30                             | 60  | 50–90                                 |
| Rb                             | 2?3  | 7                                | 17–23   | 36–70                                 |
| Sr                             | 75?111   | 193                              | 249–888   | 394–756                               |
| Y                              | 11.1?15.8  | 8.8                              | 13.4–16.0   | 14.1–20.3                             |
| Zr                             | 31?41  | 65                               | 32–53   | 74–104                                |
| Nb                             | 1.0?1.4  | 1.3                              | 1.4–2.9   | 3.0–4.2                               |
| Cs                             | 0.2?0.3  | 0.3                              | 0.4–1.3   | 0.7–5.4                               |
| Ba                             | 14?49  | 95                               | 438–585   | 456–861                               |
| La                             | 1.37?1.91  | 6.57                             | 3.33–7.11   | 14.1–24.0                             |
| Ce                             | 3.59?5.16  | 14.8                             | 8.96–18.1   | 27.8–53.4                             |
| Pr                             | 0.54?0.86  | 1.92                             | 1.27–2.49   | 3.81–6.68                             |
| Nd                             | 2.68?4.98  | 7.55                             | 5.94–10.5   | 15.8–26.2                             |
| Sm                             | 0.86?1.66  | 1.76                             | 1.61–2.46   | 3.64–5.58                             |
| Eu                             | 0.416?0.596  | 1.18                             | 0.621–0.878   | 1.28–1.68                             |
| Gd                             | 1.23?2.35  | 1.64                             | 1.74–2.45   | 3.19–4.83                             |
| Tb                             | 0.25?0.48  | 0.25                             | 0.31–0.40   | 0.50–0.68                             |
| Dy                             | 1.78?3.22  | 1.4                              | 1.90–2.29   | 2.59–3.60                             |
| Ho                             | 0.40?0.67  | 0.27                             | 0.39–0.45   | 0.48–0.67                             |
| Er                             | 1.27?2.06  | 0.77                             | 1.19–1.33   | 1.40–1.97                             |
| Tm                             | 0.201?0.324  | 0.112                            | 0.178–0.199   | 0.205–0.301                           |
| Yb                             | 1.38?2.10  | 0.77                             | 1.15–1.31   | 1.32–2.03                             |
| Lu                             | 0.225?0.325  | 0.126                            | 0.177–0.201   | 0.203–0.316                           |
| Hf                             | 0.9?1.2  | 1.8                              | 1.0–1.4   | 2.0–2.8                               |
| Ta                             | 0.06?0.71  | 0.1                              | 0.11–1.55   | 0.21–2.75                             |
| Th                             | 0.09?0.15  | 1.11                             | 0.47–1.08   | 2.08–3.92                             |
| U                              | 0.03?0.23  | 0.36                             | 0.29–0.46   | 0.63–1.36                             |

Magnesium number (Mg#) = 100 x molar Mg<sup>2+</sup>/(Mg<sup>2+</sup>+Fe<sup>2+</sup>); <sup>a</sup>From Dampare et al. (2008); <sup>b</sup>This study

contents from 47.6 to 51.8 wt.%, MgO contents from 6.85 to 8.16 wt.%,  $Al_2O_3$  contents of 12.57–14.53 wt.%, low  $TiO_2$  contents (0.62–0.82 wt.%), magnesium numbers (Mg#) of 54–60, and high contents of Cr (670–750 ppm), Ni (220–330 ppm), Co (31–70 ppm) and V (224–260). They show flat to slight LREE depletion with  $(La/Sm)_N = 0.69–1.03$ ,  $(La/Yb)_N = 0.57–0.71$ , minor negative and positive Eu anomalies ( $Eu/Eu^* = 0.92–1.24$ ), and slightly negative Nb–Ta anomalies and low Th/Nb ratios (0.06–0.11).

The Type II basalts/basaltic andesites, mainly from the Axim greenstone branch, have  $SiO_2$  contents of 48.5–52.9 wt.%, MgO contents of 3.99–12.67 wt.%,  $Al_2O_3$  contents of 10.41–16.17 wt.%,  $TiO_2$  contents of 0.54–0.86 wt.%, Mg# of 48–72, and Cr (250–1060 ppm), Ni (100–260), Co (35–42) and V (168–275). They possess fractionated REE with  $(La/Sm)_N = 1.34–2.31$ ,  $(La/Yb)_N = 2.08–4.25$  and minor positive Eu anomalies ( $Eu/Eu^* = 1.09–1.13$ ), and display strong negative Nb anomalies but relatively smaller Ti anomalies and lower Th/Nb ratios (0.35–0.37) compared to the andesites.

The andesites have variable  $SiO_2$  (56.3–63.7 wt.%), MgO (2.98–5.34 wt.%),  $Al_2O_3$  (14.2–16.8 wt.%),  $TiO_2$  (0.49–0.80 wt.%), Cr (160–270), Ni (40–120), Co (30–48), V (105–202) contents, and Mg# (40–54). They show more fractionated REE [ $(La/Sm)_N = 1.97–2.78$ ;  $(La/Yb)_N = 4.11–8.48$ ] with minor positive to non-existent Eu anomalies ( $Eu/Eu^* = 0.99–1.15$ ), and display strong negative Nb and Ti anomalies and relatively higher Th/Nb ratios (0.69–95). The dacites have  $SiO_2$  contents of 68.4–69.5%, MgO contents of 1.01–3.39 wt.%,  $Al_2O_3$  contents of 14.9–15.3 wt.%,  $TiO_2$  contents of 0.36–0.46 wt.%, and Mg# of 31–55. The analyzed dacitic porphyry has fairly high Cr (290 ppm) and Ni (130 ppm) contents, and the least contents of Co (20 ppm) and V (104). It also shows fractionated REE [ $(La/Sm)_N = 2.41$ ;  $(La/Yb)_N = 6.12$ ] with a high positive Eu anomaly ( $Eu/Eu^* = 2.12$ ), and displays strong negative Nb–Ta and Ti anomalies and a relatively high Th/Nb ratio of 0.85 (Table 1).

On the basis of Th–Nb–La–Ce systematics, Dampare et al. (2008) interpreted the negative Th and HFSE anomalies observed in the basaltic and andesitic rocks to reflect a recycled slab-derived lithosphere component instead of crustal contamination. The authors suggested that the metavolcanic rocks were formed in an intra-oceanic island arc-forearc-backarc setting.

## VII. Sr–Nd results

Sr–Nd isotopic data including  $^{87}Sr/^{86}Sr$  initial ratios,  $\epsilon_{Nd}(T)$  and Nd model ages ( $T_{DM1}$  and  $T_{DM2}$ ) are presented in Table 2. The initial  $^{87}Sr/^{86}Sr$  ratios and

$\epsilon_{Nd}$  values were calculated at an age of 2.1 Ga, which represents the crustal formation time during the Eburnean orogeny (e.g., Abouchami et al., 1990; Boher et al., 1992). The initial isotopic ratios were derived using Rb/Sr and Sm/Nd ratios from the ICP-MS data (Table 1; Dampare et al., 2008). The rocks display low  $^{87}Sr/^{86}Sr$  initial ratios (0.697637–0.702423) with the exception of one tholeiitic basalt which has a relatively higher  $^{87}Sr/^{86}Sr$  initial ratio (0.706226). The high  $^{87}Sr/^{86}Sr$  initial ratio could be due to hydrothermal alteration or a post-emplacment contamination which probably disturbed the Rb–Sr system. The low  $^{87}Sr/^{86}Sr$  initial values of D8312A (0.697637) probably suggests alteration of feldspar. The Sr initial ratios values are comparable to those previously reported on the Birimian basaltic and granitic rocks of West Africa (e.g., Abouchami et al., 1990; Boher et al., 1992; Taylor et al., 1992; Gasquet et al., 2003) (Fig. 4). These data show the primitive isotopic Sr signature of the rocks, thereby precluding significant magmatic contributions from Rb-enriched continental crust. The Type I basalts/basaltic andesites show high positive epsilon Nd (i.e., +3.89 to +7.21) isotopic initial ratios at 2.1 Ga. The andesites and Type II basalts/basaltic andesites show a range of initial  $\epsilon_{Nd}(T)$  values from –1.15 to +1.35, whereas the dacitic porphyry shows a negative initial  $\epsilon_{Nd}(T)$  value of –2.24.

Crustal residence ages ( $T_{DM}$ ) may be calculated using diverse models of depleted mantle evolution, including the models by DePaolo (1981), Ben Othman et al. (1984), Nelson and DePaolo (1985), Goldstein et al. (1984), McCulloch (1987) and Albarède and Brouxel (1987) with ages varying by several hundreds of Ma. The model of Ben Othman et al. (1984), considered to be representative of the Birimian depleted mantle and used by some workers (e.g., Abouchami et al., 1990; Boher et al., 1992; Gasquet et al., 2003), was adopted for the calculation of one-stage model ages ( $T_{DM1}$ ) of the rocks. The Nd model age of crustal rocks indicates their time of extraction from the mantle. However, the assumption that a Sm–Nd model age represents an average crustal residence time is valid only if no fractionation of Sm/Nd has taken place since the first separation of its protolith from the mantle source. Since this is not always the case and in order to avoid either underestimation or overestimation of one-stage Nd model ages, a two-stage Nd model age ( $T_{DM2}$ ) may be calculated for the rocks. The two-stage model age was computed following the procedure of Keto and Jacobson (1987), and using the expression below:

$$T_{DM2} = T_{DM1} - (T_{DM1} - t) [(f_{cc} - f_s) / (f_{cc} - f_{DM})],$$

## Sr–Nd isotopic compositions of metavolcanic rocks

Table 2

Sr–Nd isotopic compositions of Paleoproterozoic metavolcanic rocks from the southern Ashanti volcanic belt, Ghana

| Sample                  | Rb<br>(ppm) | Sr<br>(ppm) | $^{87}\text{Rb}/^{86}\text{Sr}$   | $^{87}\text{Sr}/^{86}\text{Sr}$   | 2s<br>( $\times 10^{-6}$ ) | $(^{87}\text{Sr}/^{86}\text{Sr})_{2.1}$ |                          |                          |                    |                         |
|-------------------------|-------------|-------------|-----------------------------------|-----------------------------------|----------------------------|---|--------------------------|--------------------------|--------------------|-------------------------|
| <i>Type I B/A</i>       |             |             |                                   |                                   |                            |   |                          |                          |                    |                         |
| D9045                   | <1          | 75          |                                   | 0.702447                          | 13                         |   |                          |                          |                    |                         |
| D9047                   | 2           | 111         | 0.0521                            | 0.703328                          | 11                         | 0.701751                                |                          |                          |                    |                         |
| D9048                   | 2           | 75          | 0.0772                            | 0.708562                          | 14                         | 0.706226                                |                          |                          |                    |                         |
| D9049                   | 3           | 103         | 0.0842                            | 0.70452                           | 13                         | 0.701970                                |                          |                          |                    |                         |
| <i>Type II B/A</i>      |             |             |                                   |                                   |                            |   |                          |                          |                    |                         |
| D9027                   | 23          | 249         | 0.2673                            | 0.708565                          | 10                         | 0.700475                                |                          |                          |                    |                         |
| D9028                   | 17          | 560         | 0.0878                            | 0.704000                          | 13                         | 0.701342                                |                          |                          |                    |                         |
| D9015A                  | 27          | 888         | 0.0879                            | 0.704491                          | 12                         | 0.701829                                |                          |                          |                    |                         |
| <i>Andesite</i>         |             |             |                                   |                                   |                            |   |                          |                          |                    |                         |
| D9033                   | 37          | 737         | 0.1452                            | 0.706819                          | 13                         | 0.702423                                |                          |                          |                    |                         |
| D8312                   | 70          | 394         | 0.5143                            | 0.713205                          | 14                         | 0.697637                                |                          |                          |                    |                         |
| <i>Dacitic porphyry</i> |             |             |                                   |                                   |                            |   |                          |                          |                    |                         |
| D90419                  | 7           | 193         | 0.1049                            | 0.705347                          | 12                         | 0.702171                                |                          |                          |                    |                         |
| Sample                  | Sm<br>(ppm) | Nd<br>(ppm) | $^{147}\text{Sm}/^{144}\text{Nd}$ | $^{143}\text{Nd}/^{144}\text{Nd}$ | 2s<br>( $\times 10^{-6}$ ) | $\epsilon_{\text{Nd}}$<br>(2.1 Ga)      | $T_{\text{DM1}}$<br>(Ga) | $T_{\text{DM2}}$<br>(Ga) | $f_{\text{Sm/Nd}}$ | $\alpha_{\text{Sm/Nd}}$ |
| <i>Type I B/A</i>       |             |             |                                   |                                   |                            |   |                          |                          |                    |                         |
| D9045                   | 1.66        | 4.98        | 0.2017                            | 0.513002                          | 9                          | 5.79                                    | 0.68                     | 1.92                     | 0.025              | 0.937                   |
| D9047                   | 1.40        | 4.15        | 0.2041                            | 0.513054                          | 10                         | 6.15                                    | 0.23                     | 1.91                     | 0.038              | 0.943                   |
| D9048                   | 1.29        | 3.90        | 0.2001                            | 0.513053                          | 7                          | 7.21                                    | 0.19                     | 1.83                     | 0.017              | 0.911                   |
| D9049                   | 0.86        | 2.68        | 0.1941                            | 0.512801                          | 8                          | 3.89                                    | 2.07                     | 2.09                     | -0.013             | 0.928                   |
| <i>Type II B/A</i>      |             |             |                                   |                                   |                            |   |                          |                          |                    |                         |
| D9027                   | 1.61        | 5.94        | 0.1640                            | 0.512127                          | 8                          | -1.15                                   | 3.03                     | 2.58                     | -0.166             | 0.850                   |
| D9028                   | 1.99        | 8.78        | 0.1371                            | 0.511824                          | 9                          | 0.19                                    | 2.50                     | 2.42                     | -0.303             | 0.695                   |
| D9015A                  | 2.46        | 10.5        | 0.1417                            | 0.511947                          | 7                          | 1.35                                    | 2.39                     | 2.31                     | -0.279             | 0.705                   |
| <i>Andesite</i>         |             |             |                                   |                                   |                            |   |                          |                          |                    |                         |
| D9033                   | 5.58        | 26.2        | 0.1289                            | 0.511712                          | 7                          | 0.24                                    | 2.45                     | 2.41                     | -0.345             | 0.653                   |
| <i>Dacitic porphyry</i> |             |             |                                   |                                   |                            |   |                          |                          |                    |                         |
| D90419                  | 1.76        | 7.55        | 0.1410                            | 0.511754                          | 9                          | -2.24                                   | 2.82                     | 2.64                     | -0.283             | 0.744                   |

$\epsilon_{\text{Nd}}$  values calculated at 2.1 Ga, relative to the present-day chondritic values of  $^{143}\text{Nd}/^{144}\text{Nd} = 0.512638$  and

$^{147}\text{Sm}/^{144}\text{Nd} = 0.1967$

$f_{\text{Sm/Nd}} = [(^{147}\text{Sm}/^{144}\text{Nd}_{\text{Sample}})/(^{147}\text{Sm}/^{144}\text{Nd}_{\text{CHUR}})] - 1$

$T_{\text{DM1}}$  and  $T_{\text{DM2}}$  are single-stage and two-stage Nd model ages;  $T_{\text{DM1}}$  computed according to the depleted mantle model of Ben Othman et al. (1984) and TDM2 following the approach of Keto and Jacobson (1987)

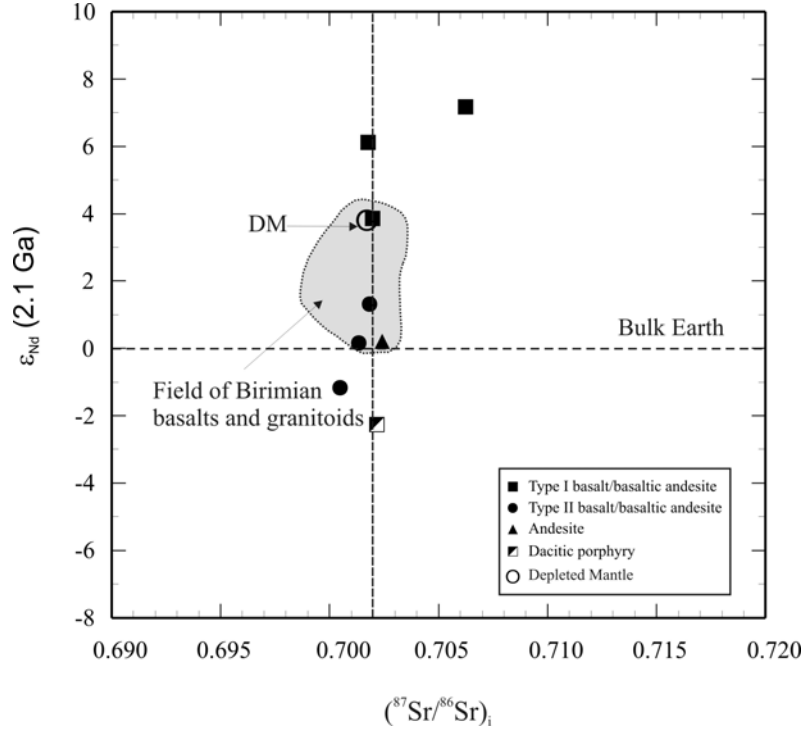


Fig. 4.  $\epsilon_{Nd}$  versus initial  $^{87}Sr/^{86}Sr$  ratios (calculated at 2.1 Ga) plot for the Paleoproterozoic metavolcanic rocks from the southern Ashanti volcanic belt. Also shown is the field of isotopic composition of Birimian basaltic and felsic rocks (shaded area) from the West African Craton (adopted from Pawling et al., 2006, and the references therein). DM represents contemporaneous depleted mantle from Ben Othman et al. (1984).

where  $f_{cc}$ ,  $f_s$  and  $f_{DM}$  are the  $f_{Sm/Nd}$  values of the continental crust, the sample and depleted mantle, respectively, and  $t$  is the formation age of the rock; and  $f_{Sm/Nd}$  is given by the expression:

$$f_{Sm/Nd} = \left[ \frac{(^{147}Sm/^{144}Nd)_{Sample}}{(^{147}Sm/^{144}Nd)_{CHUR}} \right] - 1$$

In this calculation,  $f_{cc} = -0.4$ ,  $f_{DM} = 0.086426$  and  $t = 2.1$  Ga.

Both one-stage and two-stage model ages have their own uncertainties (references in Dampare et al., 2008). Wu et al. (2005), however, indicated that more accurate results could be obtained for the single-stage model age, if the Sm/Nd fractionation, expressed as  $f_{Sm/Nd}$ , is limited to the range of  $-0.2$  to  $-0.6$ . In this study, the two-stage Nd model age ( $T_{DM2}$ ) is preferred to the single-stage model age ( $T_{DM1}$ ) as it displays a more regular pattern. The two-stage Nd model ages ( $T_{DM2}$ ) calculated for the volcanic rocks are shown in Table 2.

The model ages are 1.83–2.09 Ga for the Type I basalts/basaltic andesites, 2.31–2.58 Ga for the andesites and Type II basalts/basaltic andesites, and 2.64 Ga for the dacitic porphyry.

## VIII. Discussions

### 1. Petrogenesis

The Type I basalts/basaltic andesites (B/A) occupy a lower stratigraphic position of the volcanic pile in the study area, and they are overlain by the Type II basalts/basaltic andesites (B/A), followed by the andesites and dacites. The metavolcanic rocks were derived from a moderately depleted to slightly enriched source. The analyzed volcanic rocks commonly have low initial  $^{87}Sr/^{86}Sr$  ratios consistent with previous studies on Paleoproterozoic rocks from the West African Craton. The Type I B/A have Paleoproterozoic Nd model ages (1.83–2.09 Ga; Fig. 5), suggesting that they were juvenile at their time of formation. Their  $\epsilon_{Nd}$  (2.1 Ga) values (3.89–7.21) may suggest mantle derived magmas with variable endogenic contamination (i.e., contamination within the mantle rather than the crust, such as inputs from subducted sediments), though to a small extent. The juvenile character of these rocks is confirmed in the plot of  $\epsilon_{Nd}$  (2.1 Ga) versus formation age ( $t$ ) where they either fall in or close to the depleted mantle curve (Fig. 5),



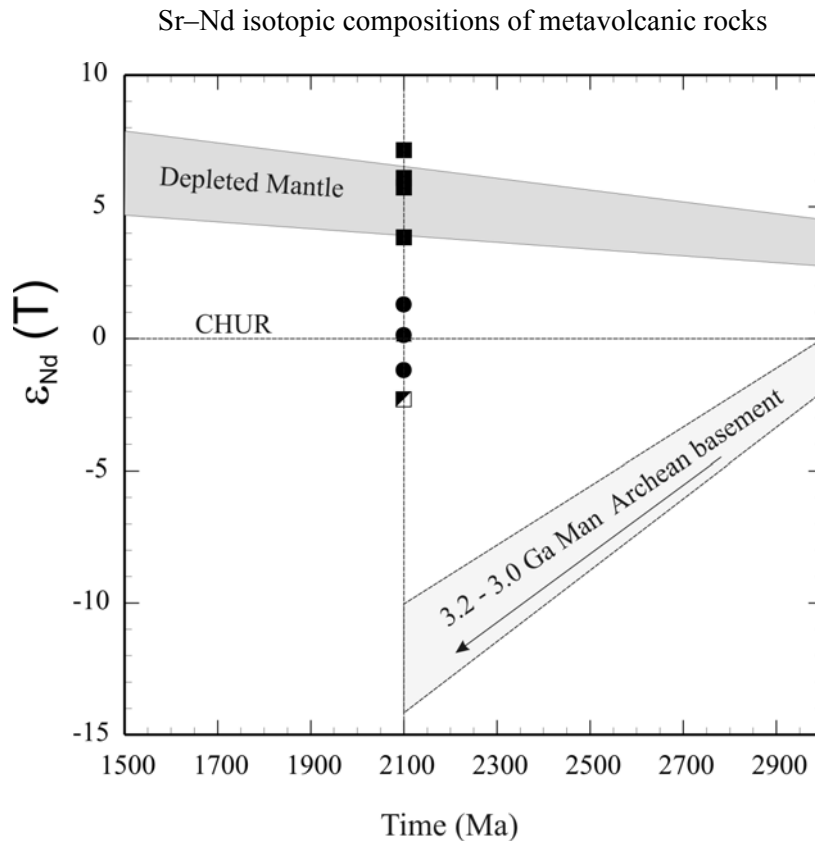


Fig. 5. Plot of  $\epsilon_{\text{Nd}}$  (2.1 Ga) versus formation age (time) for the Paleoproterozoic metavolcanic rocks from the Ashanti volcanic belt. Data of Archean continental crust is from Kouamelan et al. (1997). Symbols as in Fig. 4.

and are also widely separated from the Nd isotopic evolutionary trend of Archean crust. The Nd isotopic values used for the Archean crust are from Kouamelan et al. (1997), who estimated the composition of Archean rocks from Cote d'Ivoire which forms part of the Archean domain of the WAC, since no Archean crust is known in Ghana, at least for now. These Archean rocks have  $\epsilon_{\text{Nd}}$  (2.1 Ga) values ranging from  $-10$  to  $-13$ . As indicated earlier, the  $\epsilon_{\text{Nd}}$  (2.1 Ga) values of the plutonic rocks range from  $-5.68$  to  $+4.93$ , suggesting that the mantle source of the rocks have been contaminated to various degrees by crustal components. Thus, the trace element and isotope signatures of the Type I B/A are consistent in suggesting that their parent magma was generated from a depleted mantle. Leube et al. (1990) have indicated that most Birimian tholeiites of Ghana possess N-MORB chemistry with few showing slight to moderate LREE enrichment. The authors interpret the coexistence of both flat and LREE-enriched patterns of the tholeiites and also the  $\epsilon_{\text{Nd}}$  value of  $+2$  (Taylor et al., 1988) as indications of slight crustal contamination in the petrogenesis of the tholeiites.

The REE characteristics of the Type II B/A suggest that they could have formed from an enriched source (Dampare et al., 2008). This is consistent with their initial  $\epsilon_{\text{Nd}}$  (2.1 Ga) values from  $-1.15$  to  $+1.35$ , which are less than those of Type I B/A. Their Nd model ages  $T_{\text{DM2}}$  (2.31–2.58 Ga) are also higher than the formation age (2.1 Ga), which suggest that they may have received some inputs from crustal sources. The trace element data, however, argue against any major crustal contamination (Dampare et al., 2008). The analyzed dacitic porphyry has initial  $^{87}\text{Sr}/^{86}\text{Sr}$  ratio of 0.702171, which indicate minimum crustal contamination of the mantle melt. The  $\epsilon_{\text{Nd}}$  (2.1 Ga) values of this rock is  $-2.24$ , indicative of partly enriched to enriched mantle products. The initial  $\epsilon_{\text{Nd}}$  value of the rock coupled with geochemical features such as Nb depletion relative to the LREEs, negative Nb–Ta anomalies, relatively high LILE/HREE (or LILE/HFSE) ratios, could point to subduction-related lithospheric mantle sources. Their high negative  $\epsilon_{\text{Nd}}$  (2.1 Ga) values and Nd model age of 2.64 Ga are possibly indicative of a greater subduction input of an older crustal material. Thus, the Nd model ages of Type II B/A, andesite and dacite are dominated

by pre-Birimian (and Neoproterozoic) ages, and have received variable contributions from pre-Birimian crustal materials, with the most significant contribution recorded in the dacitic porphyry (Fig. 5). The enriched source could have resulted from a recycled slab-derived lithospheric component but not necessarily from an enriched mantle source. It is suggested that the Birimian juvenile crust was contaminated by subduction components, thereby producing heterogeneous mantle beneath the southern Ashanti volcanic belt.

The positive  $\epsilon_{Nd}$  values for some of the rocks, including those from LREE-enriched crustal precursors show that their ultimate sources had been previously depleted in Nd relative to Sm when compared to average chondritic Sm/Nd ratios. The very high positive initial  $\epsilon_{Nd}$  values (+5.79, +6.15, +7.21) for the Type I B/A indicate that mantle sources with severe time-averaged depletion probably existed in the study area. Until recently when Ngom et al. (2009) obtained an initial  $\epsilon_{Nd}$  value of +7.21 for basalt from the Mako volcanic belt of the Kedougou–Kenieba inlier (Senegal), such high initial  $\epsilon_{Nd}$  values had not been reported for the Birimian terrane of the West African craton. It can be concluded that those rocks were derived from mantle sources with a time-averaged depletion in Sm/Nd with little or no contribution from significantly older crust. The high positive initial  $\epsilon_{Nd}$  values of some of the volcanic rocks strongly suggest that the rocks were produced from the mantle entirely in an oceanic setting (cf. DePaolo, 1988).

The negative  $\epsilon_{Nd}$  (2.1 Ga) values of some of the rocks indicate that the rocks cannot be pure mantle-derived juvenile additions to the crust at 2.1 Ga, consistent with the fact that their  $T_{DM}$  ages are 200 to 540 Ma older than their emplacement age. The negative  $\epsilon_{Nd}$  (2.1 Ga) values can be explained in two possible ways: (1) they represent pure melts of crust that was formed from the mantle at 2300–2640 Ma and their  $T_{DM}$  ages faithfully record the mean crustal formation of their protolith, (2) they represent blends of juvenile 2100 Ma crust with an older component, so that their  $T_{DM}$  ages are geologically meaningless. The lack of any documented or known, at least for now, >2300 Ma geological activity in Ghana and the rest of Paleoproterozoic (Birimian) terrane of the West African craton provides an important argument against an interpretation of the rocks as pure melts of 2300–2640 Ma. The second alternative, which is a preferred model, envisages formation of the rocks by mixing of juvenile 2.1 Ga crust material with older material. The lack of correlation between the Sr and Nd isotopes (Fig. 4) makes it difficult to identify the contribution of well-defined source components in the rocks, especially those which have negative  $\epsilon_{Nd}$  (2.1 Ga) values.

### 1.1 Nd modeling: Source characteristics

The  $\epsilon_{Nd}$  values can be used to estimate the  $^{147}\text{Sm}/^{144}\text{Nd}$  ratios of the mantle source of the rocks during 2.1 Ga by using the expression (DePaolo, 1988) below:

$$f_{Sm/Nd}^{source} = \frac{\epsilon_{Nd}}{Q(T_s - T_x)}$$

where  $T_s$  = model age of the magma source and  $T_x$  = crystallization age of the rocks.

Using  $T_s = 4.55$  Ga where from accretion of the earth started,  $T_x = 2.1$  Ga,  $Q = 25.09 \text{ Ga}^{-1}$  (calculated from present day values of  $(^{147}\text{Sm}/^{144}\text{Nd})_{CHUR} = 0.1967$  and  $(^{143}\text{Nd}/^{144}\text{Nd})_{CHUR} = 0.512638$ ; Jacobsen and Wasserburg, 1984) and  $\epsilon_{Nd}$  (2.1 Ga) of the rocks, the

$f_{Sm/Nd}^{source}$  values range from -0.09 to 0.12. The  $(^{147}\text{Sm}/^{144}\text{Nd})_{source}$  of the rocks has then been computed using the relationship below:

$$f_{Sm/Nd} = \frac{(^{147}\text{Sm}/^{144}\text{Nd})_{source} - (^{147}\text{Sm}/^{144}\text{Nd})_{CHUR}}{(^{147}\text{Sm}/^{144}\text{Nd})_{CHUR}}$$

The  $(^{147}\text{Sm}/^{144}\text{Nd})_{source}$  obtained for the Type I basalts/basaltic andesites ranges from 0.209 to 0.220, which is about ~6–12% higher than the average chondrite. For the Type II basalts/basaltic andesites, the  $(^{147}\text{Sm}/^{144}\text{Nd})_{source}$  value ranges from 0.193 to 0.201, which is about ~2% lower to ~2% higher than the average chondrite. The  $(^{147}\text{Sm}/^{144}\text{Nd})_{source}$  values of the andesitic and dacitic rocks are from 0.190 to 0.197, representing ~4% lower to 0.4% higher than the average chondrite. The fractionation factor ( $\alpha$ ) was computed for the rocks using the expression of DePaolo (1988):

$$\alpha_{Sm/Nd} = \frac{1 + f_{Sm/Nd}^{rock}}{1 + f_{Sm/Nd}^{source}}$$

The  $\alpha$  values obtained for the various rocks are presented in Table 2. The  $\alpha_{Sm/Nd}$  of the Type I basalts/basaltic andesites, Type II basalts/basaltic andesites, and the andesites and dacites indicate about 6–9%, 15–31% and 26–35% depletion in the Sm/Nd ratios of the precursors of these rocks at source, respectively.

The Sm–Nd isotopic modeling suggests that the volcanic were derived from heterogeneous mantle sources.

## 2. Tectonic setting

The geotectonic environment in which the rocks were formed or emplaced was investigated in the plot of  $f_{Sm/Nd}$  versus  $\epsilon_{Nd}$  (2.1 Ga). The Type I basalts/basaltic andesites plot in the field of MORB but close to the arc crust. Indeed, their  $\epsilon_{Nd}$  (2.1 Ga) values overlap the fields of Paleoproterozoic arc crust and MORB (Fig.

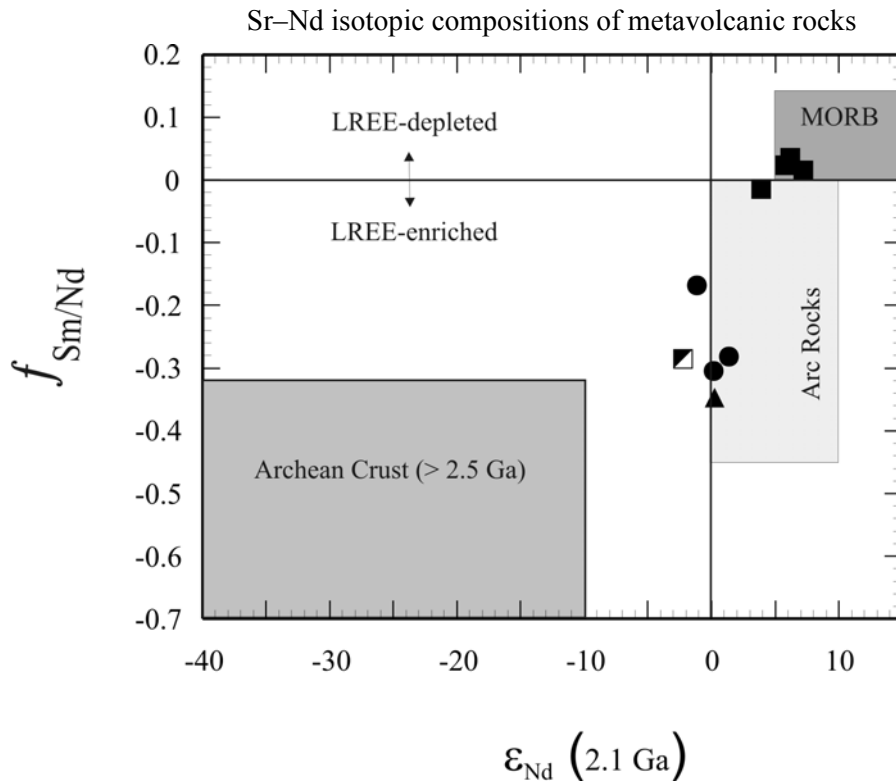


Fig. 6. Plot of  $\epsilon_{\text{Nd}}(2.1 \text{ Ga})$  versus fractionation parameter ( $f_{\text{Sm/Nd}}$ ). Fields of old (Archean) continental crust, MORB and the arc rocks are from Roddaz et al. (2007) and the references therein. Symbols as in Fig. 4.

6; Roddaz et al., 2000 and the references therein). The Type II basalts/basaltic andesites, andesites and dacites are either plotted in and close to the field of the Proterozoic arc crust.

The geotectonic setting of the Paleoproterozoic rocks of Ghana is contentious. Leube et al. (1990) have proposed an intracrustal rift model for the Paleoproterozoic rocks, whereas arc or subduction related models have been suggested by others (Sylvester and Attoh, 1992; Pohl and Carlson, 1993; Loh and Hirdes, 1999; Asiedu et al., 2004; Dampare et al., 2005; Attoh et al., 2006; Dampare et al., 2008, in review). Feybesse et al. (2006) have invoked a combination of continental margin, juvenile magmatism and convergence and collision between an old continent and a juvenile crust for the tectonic environments in which the Birimian greenstone belts were generated. For Harcouet et al. (2007), the basement in the Ashanti area is likely to be of continental type rather than oceanic, as the results of their numerical modeling using thermal parameters such as thermal conductivity values and heat-production rates are more consistent with the continental basement scenario. Sylvester and Attoh (1992) have indicated that the trace element chemistry

of Birimian volcanic belts in Ghana is comparable to that of Archean greenstone belts, and that intermediate calc-alkaline units show the high Ba/La and Ta depletion which is characteristic of similar rocks in modern subduction environments and distinct from those formed in intraplate settings. The authors therefore suggest that Birimian volcanic rocks probably originated as immature island arcs built on oceanic crust. Dampare et al. (2008) have, on the basis of geochemistry, inferred an intra-oceanic island arc–fore-arc–back-arc setting for the Paleoproterozoic metavolcanic rocks from the southern Ashanti volcanic belt. The formation of most of the Paleoproterozoic volcanic belts in the oceanic context has also been underlined by other workers (e.g., Abouchami et al., 1990; Liégeois et al. 1991; Boher et al., 1992; Davis et al., 1994; Vidal and Alric, 1994; Ama Salah et al., 1996; Béziat et al. 2000; Egal et al., 2002). Available geochronological and isotopic data (e.g., Abouchami et al. 1990; Liégeois et al. 1991; Boher et al. 1992; Taylor et al. 1992; Hirdes et al. 1996; Ama Salah et al. 1996; Doumbia et al. 1998; Gasquet et al. 2003) indicate a juvenile source for the Paleoproterozoic volcanic and granitic rocks, with the exceptions of plutons from the Winneba area in the southeast of

Ghana (Taylor et al., 1992) and the vicinity of the Man nucleus (e.g., Kouamelan et al., 1997), where there is evidence of a stronger influence of recycled Archean basement.

Abouchami et al. (1990) and Boher et al. (1992) have proposed a mantle plume model to explain crustal growth event in the West African Craton. According to the authors, extensive plateaus were formed by a mantle plume event, followed by formation of island arcs on the top of the oceanic plateaus which then collided with the Man Archean Craton. For the crustal growth event in Ghana, Taylor et al. (1992) have indicated that the Birimian represents a major early Proterozoic magmatic crust-forming event around 2.3–2.0 Ga by differentiation from a slightly depleted mantle source. The authors suggest that the Birimian of Ghana forms part of the major Proterozoic (Eburnean) episode of juvenile crustal accretion which is recognized in West African Craton and dated at 2.2–2.1 Ga by Abouchami et al. (1990). Davis et al. (1994), also following the accretionary model, have proposed that the Birimian sedimentary basins resulted from accretion of arcs and oceanic plateaus now represented by allochthonous Birimian volcanic belts. For Feybesse et al. (2006) the Birimian volcanic belts correspond to a major period of accretion of juvenile basic volcanic–plutonic rocks to an Archean continental domain around 2.25–2.17 Ga, whereas the Birimian sedimentary activity occurred at 2.15–2.10 Ga (Feybesse et al., 2006).

Our isotopic data favors a supra-subduction magmatism in the study area, consistent with the previously published geochemical data on the metavolcanics (Dampare et al., 2008) but inconsistent with the mantle plume model proposed for Paleoproterozoic rocks in Ghana (e.g., Leube et al., 1990). This is consistent with the island arc complex model that the Paleoproterozoic terranes of West Africa evolved through subduction-accretion processes.

## IX. Conclusion

The metavolcanic rocks analyzed in this work are predominantly basalts/basaltic andesites and andesites with minor dacites. Two main basalts/basaltic andesites (B/A) have been identified, and are subsequently referred to as Type I B/A and Type II B/A. The tholeiitic Type I B/A are underlain by the calc-alkaline Type II B/A, andesites and dacites.

The analyzed metavolcanic rocks generally have low initial  $^{87}\text{Sr}/^{86}\text{Sr}$  ratios values comparable to those previously reported on the Birimian basaltic and granitic rocks of West Africa. The isotope signatures of the Type I B/A suggest that their parent magma was

derived from a depleted mantle source. They show high positive initial  $\epsilon_{\text{Nd}}(T)$ , i.e., +3.89 to +7.21. The wide range of epsilon values suggests some contribution from endogenic sources. The Type I B/A display Nd model ages ( $T_{\text{DM2}}$ ) of 1.83–2.09 Ga similar to their formation ages, suggesting that they were juvenile at their time of formation. The andesites and Type II basalts/basaltic andesites show a range of  $\epsilon_{\text{Nd}}(2.1 \text{ Ga})$  values from –1.15 to +1.35, which are less than those of Type I B/A. Their Nd model ages ( $T_{\text{DM2}} = 2.31–2.58 \text{ Ga}$ ) are also higher than the formation age (2.1 Ga), which suggest that they may have received some inputs from crustal sources. The andesites and andesites and dacites show a range of initial  $\epsilon_{\text{Nd}}(T)$  values from –2.24 to +0.24, indicative of much higher crustal inputs or partly enriched to enriched mantle products. The initial  $\epsilon_{\text{Nd}}$  value of the rock coupled with geochemical features could point to subduction-related lithospheric mantle sources. Their pre-Birimian Nd model age of 2.41–2.64 Ga are possibly indicative of a greater subduction input of an older crustal material. The trace element data, of the metavolcanic rocks argue against any major crustal contamination (Dampare et al., 2008). Therefore, the isotopic heterogeneities demonstrated by the rocks may probably be due to variable endogenic contamination (i.e., contamination within the mantle rather than the crust, such as inputs from subducted sediments).

The radiogenic isotopic signatures are consistent with the trace element data in suggesting a supra-subduction zone setting for the metavolcanic rocks from the study area. The Type I basalts/basaltic andesites were generated from a depleted mantle in a back-arc basin, whereas the arc-related Type I B/A, andesites and dacites were derived from heterogeneous, metasomatized lithospheric mantle sources. The isotopic signatures of the metavolcanic rocks support supra-subduction magmatism in the southern Ashanti greenstone belt of Ghana.

## Acknowledgements

The field work was partly sponsored by the National Nuclear Research Institute (NNRI) of Ghana Atomic Energy Commission. The first author gratefully acknowledges the financial support received from the Japanese Government (Monbukagakusho: MEXT).

## References

- Abouchami, W., Boher, M., Michard, A. and Albarade, F. (1990) A major 2.1 Ga event of mafic magmatism



## Sr–Nd isotopic compositions of metavolcanic rocks

- in West Africa: an early stage of crustal accretion. *J. Geophys. Res.*, **95**, 17605–17629.
- Albarède, F. and Brouxel, M. (1987) The Sm–Nd secular evolution of the continental crust and the depleted mantle. *Earth Planet. Sci. Lett.*, **82**, 25–36.
- Allibone, A., McCuaig, C.T., Harris, D., Etheridge M., Munroe, S., Byrne, D., Amanor, J. and Gyapong, W. (2002) Structural controls on gold mineralization at the Ashanti Gold Deposit, Obuasi, Ghana. In: *Integrated Methods for Discovery: Global Exploration in the 21st Century* (Goldfarb, R.J. and Neilson, R.L., Eds.), Society of Economic Geologists Special Publication **9**, pp. 65–93.
- Ama Salah, I., Liégeois, J.-P. and Pouclet, A. (1996) Evolution d'un arc insulaire océanique birimian précoce au Liptako nigérien (Sirba): géologie, géochronologie et géochimie. *J. Afr. Earth Sci.*, **22**, 235–254.
- Asiedu, D.K., Dampare, S.B., Asamoah, S. P., Banoeng-Yakubo, B., Osaë, S., Nyarko, B.J.B. and Manu, J. (2004) Geochemistry of Paleoproterozoic metasedimentary rocks from the Birim diamondiferous field, southern Ghana: implications for provenance and crustal evolution at the Archean–Proterozoic boundary. *Geochem. J.*, **38**, 215–228.
- Attoh, K., Evans, M.J. and Bickford, M.E. (2006) Geochemistry of an ultramafic-rodinigte rock association in the Paleoproterozoic Dixcove greenstone belt, southwestern Ghana. *J. Afr. Earth Sci.* **45**, 333–346.
- Bartholomew, R.W. (1961) The geology of 1/4° field sheets 3 and 5 Axim NE,1. pp. 78, Ghana Geol. Surv. Arch. Rep. 18 (1991), Accra.
- Bassot, J.P. (1987) Le complexe volcano-plutonique calcoalcalin de la rive'ère Daléma (Est Sénégal): discussion de sa signification géodynamique dans le cadre de l'orogénie eburnéenne (Protérozoic inférieur). *J. Afr. Earth Sci.*, **6**, 505–519.
- Ben Othman, D., Polvé, M. and Allègre, C.J. (1984) Nd–Sr isotopic composition of granulites and constraints on the evolution of the lower continental crust. *Nature*, **307**, 510–515.
- Béziat, D., Bourges, F., Debat, P., Lompo, M., Martin, F. and Tollon, F. (2000) A Paleoproterozoic ultramafic–mafic assemblage and associated volcanic rocks of the Boromo greenstone belt: fractionates originating from island-arc volcanic activity in the West African craton. *Precambrian Res.*, **101**, 25–47.
- Blenkinsop, T., Schmidt Mumm, A., Kumi, R. and Sangmor, S. (1994), Structural geology of the Ashanti gold mine. *Geologisches Jahrbuch*, **D100**, 131–153.
- Boher, M., Abouchami, W., Michard, A., Albarrede, F. and Arnt, N.T. (1992) Crustal growth in West Africa at 2.1 Ga. *J. Geophys. Res.*, **95**, 345–369.
- Dampare, S., Shibata, T., Asiedu, D. and Osaë, S. (2005) Major-element geochemistry of Proterozoic Prince's Town granitoid from the southern Ashanti volcanic belt, Ghana. *Okayama Univ. Earth Sci. Reports*, **12**, 15–30.
- Dampare, S.B. (2008) Petrology and geochemistry of Paleoproterozoic mafic–ultramafic bodies and associated volcanic rocks in the southern part of the Ashanti greenstone belt, Ghana. pp. 241, Ph.D. thesis, Okayama University.
- Dampare, S.B., Shibata, T., Asiedu, D.K., Okano, O., Osaë, S. and Atta-Peters, D. (in review) Mafic and ultramafic supra-subduction magmatism in the Ashanti volcanic belt, Ghana: evidence from geochemistry and Nd isotopes. *Precambrian Res.*
- Dampare, S.B., Shibata, T., Asiedu, D.K., Osaë, S. and Banoeng-Yakubo, B. (2008) Geochemistry of Paleoproterozoic metavolcanic rocks from the southern Ashanti volcanic belt, Ghana: petrogenetic and tectonic setting implications. *Precambrian Res.*, **162**, 403–423.
- Davis, D.W., Hirdes, W., Schaltegger, U. and Nunoo, E.A. (1994) U–Pb age constraints on deposition and provenance of Birimian and gold-bearing Tarkwaian sediments in Ghana, West Africa. *Precambrian Res.*, **67**, 89–1207.
- Debat, P., Nikiema, S., Mercier, A., Lompo, M., Beziat, D., Bourges, F., Roddaz, M., Salvi, S., Tollon, F. and Wenmenga, U. (2003) A new metamorphic constraint for the Eburnean orogeny from Paleoproterozoic formations of the Man shield (Aribinda and Tampilga countries, Burkina Faso). *Precambrian Res.*, **123**, 47–65.
- DePaolo, D.J. (1981) Neodymium isotopes in the Colorado Front Range and crust-mantle evolution in the Proterozoic. *Nature (London)*, **291**, 193–196.
- DePaolo, D.J. (1988) *Neodymium isotope geochemistry. An introduction*. pp. 187, Springer, Berlin.
- DePaolo, D.J., Linn, A.M. and Schubert, G. (1991) The continental crust age distribution: methods of determining mantle separation ages from Sm–Nd isotopic data and implication to the southwestern United States. *J. Geophys. Res.*, **96** (B2), 2071–2088.
- Doumbia, S., Pouclet, A., Kouamelan, A., Peucat, J.J., Vidal, M. and Delor, C. (1998) Petrogenesis of juvenile-type Birimian (Palaeoproterozoic) granitoids in Central Côte d'Ivoire, West Africa: geochemistry and geochronology. *Precambrian Res.*, **87**, 33–63.

- Egal, E., Thiéblemont, D., Lahondère, D., Guerrot, C., Costea, C.A., Iliescu, D., Delor, C., Goujou, J.-C., Lafon, J.M., Tegye, M., Diaby, S. and Kolié, P. (2002) Late Eburnean granitization and tectonics along the western and northwestern margin of the Archean Kénéma–Man domain (Guinea, West African Craton). *Precambrian Res.*, **117**, 57–84.
- Eisenlohr, B.N. (1992) Conflicting evidence on the timing of mesothermal and paleoplacer gold mineralization in early Proterozoic rocks from Southwest Ghana, West Africa. *Miner. Deposita*, **27**, 23–29.
- Eisenlohr, B.N. and Hirdes, W. (1992) The structural development of the early Proterozoic Birimian and Tarkwaian rocks of southwest Ghana, West Africa. *J. Afr. Earth Sci.*, **14**, 313–325.
- Feybesse, J.L. and Milési, J.P. (1994) The Archean/proterozoic contact zone in West Africa: a mountain belt of décollement thrusting and folding on a continental margin related to 2.1 Ga convergence of Archean cratons? *Precambrian Res.*, **69**, 199–227.
- Feybesse, J.L., Billa, M., Guerrot, C., Duguey, E., Lescuyer, J.L., Jean-Pierre Milési, J.P. and Bouchot, V. (2006) The paleoproterozoic Ghanaian province: geodynamic model and ore controls, including regional stress modeling. *Precambrian Res.*, **149**, 149–196.
- Gasquet, D., Barbey, P., Adou, M. and Paquette, J.L. (2003) Structure, Sr–Nd isotope geochemistry and zircon U–Pb geochronology of the granitoids of the Dabakala area (Côte d’Ivoire): evidence for a 2.3 Ga crustal growth event in the Paleoproterozoic of West Africa? *Precambrian Res.*, **127**, 329–354.
- Goldstein, S.L., O’Nions, R.K. and Hamilton, P.J. (1984) A Sm–Nd isotopic study of atmospheric dusts and particulate from major river systems. *Earth Planet. Sci. Lett.*, **70**, 221–236.
- Harcouët, V., Guillou-Frottier, L., Bonneville, A., Bouchot, V. and Milesi, J.-P. (2007) Geological and thermal conditions before the major Palaeoproterozoic gold-mineralization event at Ashanti, Ghana, as inferred from improved thermal modeling. *Precambrian Res.*, **154**, 71–87.
- Hirdes, W. and Davis, D.W. (2002) U–Pb geochronology of Paleoproterozoic rocks in the southern part of the Keougou-Keneba inlier, Senegal, West Africa: evidence for diachronous accretionary development of the Birimian Province. *Precambrian Res.*, **118**, 83–99.
- Hirdes, W., Davis, D.W. and Eisenlohr, B.N. (1992) Reassessment of Proterozoic of Proterozoic granitoid ages in Ghana on the basis of U/Pb zircon and monzanite dating. *Precambrian Res.*, **56**, 89–96.
- Hirdes, W., Davis, D.W., Lüdtke, G. and Konan, G. (1996) Two generations of Birimian (Paleoproterozoic volcanic belts in northeastern Côte d’Ivoire (West Africa): consequences for the ‘Birimian controversy’. *Precambrian Res.*, **80**, 173–191.
- Hirdes, W., Senger, R., Adjei, J., Efa, E., Loh, G. and Tettey, A. (1993) Explanatory notes for the geological map of southwest Ghana: 1:1000000. *Geologisches Jahrbuch*, **83**, 5–139.
- Jacobsen, S.B. and Wasserburg, G.J. (1984) Sm–Nd isotopic evolution of chondrites and achondrites, II. *Earth Planet. Sci. Lett.*, **67**, 137–150.
- John, T., Klemd, R., Hirdes, W. and Loh, G. (1999) The metamorphic evolution of the Paleoproterozoic (Birimian) volcanic Ashanti belt (Ghana, West Africa). *Precambrian Res.*, **98**, 11–30.
- Junner, N.R. (1935) Gold in the Gold Coast. Mem., pp. 67, Gold Coast Geol. Surv. (4), Accra.
- Junner, N.R. (1940) Geology of the Gold Coast and Western Togoland (with revised geological map), pp. 40, Bull. Gold Coast Geol. Surv. (11), Accra.
- Kesse, G.O. (1985) *The mineral and rock resources of Ghana*. 610pp, Balkema, Rotterdam.
- Keto, L.S. and Jacobsen, S.B. (1987) Nd and Sr isotopic variations of early Paleozoic oceans. *Earth Planet. Sci. Lett.*, **84**, 27–41.
- Kouamelan, A.N., Delor, C. and Peucat, J.-J. (1997) Geochronological evidence for reworking of Archean terrains during the Early Proterozoic (2.1 Ga) in the western Cote d’Ivoire (Man Rise–West African Craton). *Precambrian Res.*, **86**, 177–199.
- Ledru, P., Johan, V., Milési, J.P. and Tegye, M. (1994) Markers of the last stages of the Palaeoproterozoic collision: evidence for a 2 Ga continent involving circum-South Atlantic provinces. *Precambrian Res.*, **69**, 169–191.
- Ledru, P., Milesi, J.-P., Vinchon, C., Ankrah, P.T., Johan, V. and Marcoux, E. (1988) Geology of the Birimian series of Ghana. In: International Conference and Workshop on the Geology of Ghana with Special Emphasis on Gold Programme and Abstracts, Accra, Ghana, pp. 26–27.
- Leube, A., Hirdes, W., Mauer, R. and Kesse, G.O. (1990) The Early Proterozoic Birimian Supergroup of Ghana and some aspects of its associated gold mineralization. *Precambrian Res.*, **46**, 139–165.
- Liégeois, J.P., Claessens, W., Camara, D. and Klerkx, J. (1991) Short-lived Eburnean orogeny in southern Mali: geology, tectonics, U–Pb and Rb–Sr geochronology. *Precambrian Res.*, **50**, 111–136.
- Loh, G. and Hirdes, W. (1999) Geological map of southwest Ghana, 1:100000, sheets Sekondi

## Sr–Nd isotopic compositions of metavolcanic rocks

- (0402A) and Axim (0403B), pp. 149, Bull. Ghana Geol. Surv. (49), Hannover.
- Lompo, M. (2009) Geodynamic evolution of the 2.25–2.0 Ga Palaeoproterozoic magmatic rocks in the Man-Leo Shield of the West African Craton. A model of subsidence of an oceanic plateau. In: Palaeoproterozoic Supercontinents and Global Evolution (Reddy, S.M., Mazumder, R., Evans, D.A.D. and Collins, A.S., Eds.), Geological Society of London Special Publication, **323**, pp. 231–254.
- McCulloch, M.T. (1987) Sm–Nd isotopic constraints on the evolution of Precambrian crust in the Australian continent. In: Proterozoic Lithospheric Evolution (Kröner, A., Ed.), Geodyn. Ser., vol. 17, AGU, Washington, D.C., pp. 115–130.
- Milési, J.P., Ledru, P., Feybesse, J.L., Dommange, A. and Marcoux, E. (1992) Early Proterozoic ore deposits and tectonics of the Birimian orogenic belt, West Africa. *Precambrian Res.*, **58**, 305–344.
- Moon, P.A. and Mason, D. (1967) The geology of the 1°/4 field sheets Nos. 129 and 131, Bompata SW and NW, pp. 51, Geol. Surv. Ghana Bull. (31), Accra.
- Mortimer, J. (1992) Lithostratigraphy of the early Proterozoic Toumodi Volcanic Group in Central Côte d’Ivoire: implications for Birimian stratigraphy models. *J. Afr. Earth Sci.*, **14**, 81–91.
- Mumin, A.H. and Fleet, M.E. (1995) Evolution of gold mineralization in the Ashanti gold belt, Ghana: evidence from carbonate compositions and paragenesis. *Miner. Petrol.*, **81**, 268–276.
- Nelson, B.K. and DePaolo, D.J. (1985) Rapid production of continental crust 1.7 to 1.9 b.y. ago: Nd isotopic evidence from the basement of the North America mid continent. *Geol. Soc. Am. Bull.*, **96**, 746–754.
- Ngom, P.M., Cordani, U.G., Teixeira, W. and Janasi, V.d.A (in press) Sr and Nd isotopic geochemistry of the early ultramafic–mafic rocks of the Mako bimodal volcanic belt of the Kedougou–Kenieba inlier (Senegal). *Arab. J. Geosci.*, DOI 10.1007/s12517-009-0051-3.
- Oberthür, T., Schmidt Mumm, A., Vetter, U., Simon, K. and Amanor, J.A. (1996), Gold mineralization in the Ashanti belt of Ghana: genetic constraints of stable isotope geochemistry. *Econ. Geol.*, **91**, 289–301.
- Oberthür, T., Vetter, U., Davis, D.W., Amanor, J.A. (1998) Age constraints on gold mineralization and Paleoproterozoic crustal evolution in the Ashanti belt of southern Ghana. *Precambrian Res.*, **89**, 129–143.
- Opore-Addo, E., Browning, P. and John, B.E. (1993) Pressure-temperature constraints on the evolution of an early Proterozoic plutonic suite in southern Ghana, West Africa. *J. Afr. Earth Sc.*, **17**, 13–22.
- Patchett, P.J. and Arndt, N.T. (1986) Nd isotope and tectonics of 1.9–1.7 crustal genesis. *Earth Planet. Sci. Lett.*, **78**, 329–338.
- Pawlig, S., Gueye, M., Klischies, R., Schwarz, S., Wemmer, K. and Siegesmund, S. (2006) Geochemical and Sr–Nd isotopic data on the Birimian of the Kedougou–Kenieba Inlier (Eastern Senegal): Implications on the Palaeoproterozoic evolution of the West African Craton. *S. Afr. J. Geol.*, **109**, 411–427.
- Pigois, J.-P., Groves, D.I., Fletcher, I.R., McNaughton, N.J. and Snee, L.W. (2003) Age constraints on Tarkwaian palaeoplacer and lode-gold formation in the Tarkwa–Damang district, SW Ghana. *Miner. Deposita*, **38**, 695–714.
- Pohl, D. and Carlson, C. (1993) A plate tectonic re-interpretation of the 2.2–2.0 Ga Birimian province, Tarkwaian System and metallogenesis in West Africa. In: Regional Trends in African Geology (Peters, J.W., Kesse, G.O. and Acquah, P.C., Eds.), Geol. Soc. Africa, Accra, 378–381.
- Poucllet, A., Vidal, M., Delor, C., Simeon, Y. and Alric, G. (1996) Le volcanisme birimien de la Cote d’Ivoire, mise en évidence de deux phases volcano-tectoniques distinctes dans l’évolution géodynamique du Paléoproterozoïque. *Bull. Soc. Geol. France*, **167**, 529–541.
- Roddaz, M., Debat, P. and Nikiéma, S. (2007) Geochemistry of Upper Birimian sediments (major and trace elements and Nd–Sr isotopes) and implications for weathering and tectonic setting of the Late Paleoproterozoic crust. *Precambrian Res.*, **159**, 197–211.
- Sylvester, P.J. and Atttoh, K. (1992) Lithostratigraphy and composition of 2.1 Ga greenstone belts of the West African Craton and their bearing on crustal evolution and the Archean–Proterozoic boundary. *J. Geol.*, **100**, 377–393.
- Tagini, B. (1971) Esquisse structurale de la Cote d’Ivoire. Essai de géotectonique régionale. pp. 302, These Univ. Lausanne. Soc. Dev. Min. Cote d’Ivoire (SODEMI).
- Taylor, P.N., Moor bath, S., Leube, A. and Hirdes, W. (1988) Geochronology and crustal evolution of Early Proterozoic granite-greenstone terrains in Ghana/West Africa. Abstr., International Conference on the geology of Ghana with special emphasis on Gold. 75th Anniversary of Ghana Geol. Surv. Dept., Accra, pp. 43–45.
- Taylor, P.N., Moor bath, S., Leube, A. and Hirdes, W. (1992) Early Proterozoic crustal evolution in the Birimian of Ghana: constraints from geochronology and isotope geology. *Precambrian Res.*, **56**, 97–111.

- Tunks, A.J., Selley, D., Rogers, J.R. and Brabham, G. (2004) Vein mineralization at the Damang Gold Mine, Ghana: controls on mineralization. *J. Struct. Geol.*, **26**, 1257–1273.
- Vidal, M. and Alric, G. (1994) The Palaeoproterozoic (Birimian) of Haute-Comoé in the West African craton, Ivory Coast: a transtensional back-arc basin. *Precambrian Res.*, **65**, 207–229.
- Wu, F., Zhao, G., Simon A. Wilde, S.A. and Sun, D. (2005) Nd isotopic constraints on crustal formation in the North China Craton. *J. Asian Earth Sci.*, **24**, 523–545.
- Yao, Y., Murphy, P.J. and Robb, L.J. (2001) Fluid characteristics of granitoid-hosted gold deposits in the Birimian Terrane of Ghana: a fluid inclusion microthermometric and Raman spectroscopic study. *Econ. Geol.*, **96**, 1611–1643.